

PDF hosted at the Radboud Repository of the Radboud University Nijmegen

The following full text is a postprint version which may differ from the publisher's version.

For additional information about this publication click this link.

<http://hdl.handle.net/2066/72636>

Please be advised that this information was generated on 2021-06-24 and may be subject to change.

Measurement of the ratios of the $Z/\gamma^* + \geq n$ jet production cross sections to the total inclusive Z/γ^* cross section in $p\bar{p}$ collisions at $\sqrt{s} = 1.96$ TeV

V.M. Abazov,³⁶ B. Abbott,⁷⁶ M. Abolins,⁶⁶ B.S. Acharya,²⁹ M. Adams,⁵² T. Adams,⁵⁰ M. Agelou,¹⁸ S.H. Ahn,³¹ M. Ahsan,⁶⁰ G.D. Alexeev,³⁶ G. Alkhazov,⁴⁰ A. Alton,⁶⁵ G. Alverson,⁶⁴ G.A. Alves,² M. Anastasoiaie,³⁵ T. Andeen,⁵⁴ S. Anderson,⁴⁶ B. Andrieu,¹⁷ M.S. Anzels,⁵⁴ Y. Arnold,¹⁴ M. Arov,⁵³ A. Askew,⁵⁰ B. Åsman,⁴¹ A.C.S. Assis Jesus,³ O. Atramentov,⁵⁸ C. Autermann,²¹ C. Avila,⁸ C. Ay,²⁴ F. Badaud,¹³ A. Baden,⁶² L. Bagby,⁵³ B. Baldin,⁵¹ D.V. Bandurin,⁶⁰ P. Banerjee,²⁹ S. Banerjee,²⁹ E. Barberis,⁶⁴ P. Bargassa,⁸¹ P. Baringer,⁵⁹ C. Barnes,⁴⁴ J. Barreto,² J.F. Bartlett,⁵¹ U. Bassler,¹⁷ D. Bauer,⁴⁴ A. Bean,⁵⁹ M. Begalli,³ M. Begel,⁷² C. Belanger-Champagne,⁵ L. Bellantoni,⁵¹ A. Bellavance,⁶⁸ J.A. Benitez,⁶⁶ S.B. Beri,²⁷ G. Bernardi,¹⁷ R. Bernhard,⁴² L. Berntzon,¹⁵ I. Bertram,⁴³ M. Besançon,¹⁸ R. Beuselinck,⁴⁴ V.A. Bezzubov,³⁹ P.C. Bhat,⁵¹ V. Bhatnagar,²⁷ M. Binder,²⁵ C. Biscarat,⁴³ K.M. Black,⁶³ I. Blackler,⁴⁴ G. Blazey,⁵³ F. Blekman,⁴⁴ S. Blessing,⁵⁰ D. Bloch,¹⁹ K. Bloom,⁶⁸ U. Blumenschein,²³ A. Boehnlein,⁵¹ O. Boeriu,⁵⁶ T.A. Bolton,⁶⁰ G. Borissov,⁴³ K. Bos,³⁴ T. Bose,⁷⁸ A. Brandt,⁷⁹ R. Brock,⁶⁶ G. Brooijmans,⁷¹ A. Bross,⁵¹ D. Brown,⁷⁹ N.J. Buchanan,⁵⁰ D. Buchholz,⁵⁴ M. Buehler,⁸² V. Buescher,²³ S. Burdin,⁵¹ S. Burke,⁴⁶ T.H. Burnett,⁸³ E. Busato,¹⁷ C.P. Buszello,⁴⁴ J.M. Butler,⁶³ P. Calfayan,²⁵ S. Calvet,¹⁵ J. Cammin,⁷² S. Caron,³⁴ W. Carvalho,³ B.C.K. Casey,⁷⁸ N.M. Cason,⁵⁶ H. Castilla-Valdez,³³ D. Chakraborty,⁵³ K.M. Chan,⁷² A. Chandra,⁴⁹ F. Charles,¹⁹ E. Cheu,⁴⁶ F. Chevallier,¹⁴ D.K. Cho,⁶³ S. Choi,³² B. Choudhary,²⁸ L. Christofek,⁵⁹ D. Claes,⁶⁸ B. Clément,¹⁹ C. Clément,⁴¹ Y. Coadou,⁵ M. Cooke,⁸¹ W.E. Cooper,⁵¹ D. Coppage,⁵⁹ M. Corcoran,⁸¹ M.-C. Cousinou,¹⁵ B. Cox,⁴⁵ S. Crépe-Renaudin,¹⁴ D. Cutts,⁷⁸ M. Cwiok,³⁰ H. da Motta,² A. Das,⁶³ M. Das,⁶¹ B. Davies,⁴³ G. Davies,⁴⁴ G.A. Davis,⁵⁴ K. De,⁷⁹ P. de Jong,³⁴ S.J. de Jong,³⁵ E. De La Cruz-Burelo,⁶⁵ C. De Oliveira Martins,³ J.D. Degenhardt,⁶⁵ F. Déliot,¹⁸ M. Demarteau,⁵¹ R. Demina,⁷² P. Demine,¹⁸ D. Denisov,⁵¹ S.P. Denisov,³⁹ S. Desai,⁷³ H.T. Diehl,⁵¹ M. Diesburg,⁵¹ M. Doidge,⁴³ A. Dominguez,⁶⁸ H. Dong,⁷³ L.V. Dudko,³⁸ L. Duflot,¹⁶ S.R. Dugad,²⁹ D. Duggan,⁵⁰ A. Duperrin,¹⁵ J. Dyer,⁶⁶ A. Dyshkant,⁵³ M. Eads,⁶⁸ D. Edmunds,⁶⁶ T. Edwards,⁴⁵ J. Ellison,⁴⁹ J. Elmsheuser,²⁵ V.D. Elvira,⁵¹ S. Eno,⁶² P. Ermolov,³⁸ H. Evans,⁵⁵ A. Evdokimov,³⁷ V.N. Evdokimov,³⁹ S.N. Fatakia,⁶³ L. Feligioni,⁶³ A.V. Ferapontov,⁶⁰ T. Ferbel,⁷² F. Fiedler,²⁵ F. Filthaut,³⁵ W. Fisher,⁵¹ H.E. Fisk,⁵¹ I. Fleck,²³ M. Ford,⁴⁵ M. Fortner,⁵³ H. Fox,²³ S. Fu,⁵¹ S. Fuess,⁵¹ T. Gadfort,⁸³ C.F. Galea,³⁵ E. Gallas,⁵¹ E. Galyaev,⁵⁶ C. Garcia,⁷² A. Garcia-Bellido,⁸³ J. Gardner,⁵⁹ V. Gavrilov,³⁷ A. Gay,¹⁹ P. Gay,¹³ D. Gelé,¹⁹ R. Gelhaus,⁴⁹ C.E. Gerber,⁵² Y. Gershtein,⁵⁰ D. Gillberg,⁵ G. Ginter,⁷² N. Gollub,⁴¹ B. Gómez,⁸ A. Goussiou,⁵⁶ P.D. Grannis,⁷³ H. Greenlee,⁵¹ Z.D. Greenwood,⁶¹ E.M. Gregores,⁴ G. Grenier,²⁰ Ph. Gris,¹³ J.-F. Grivaz,¹⁶ S. Grünendahl,⁵¹ M.W. Grünewald,³⁰ F. Guo,⁷³ J. Guo,⁷³ G. Gutierrez,⁵¹ P. Gutierrez,⁷⁶ A. Haas,⁷¹ N.J. Hadley,⁶² P. Haefner,²⁵ S. Hagopian,⁵⁰ J. Haley,⁶⁹ I. Hall,⁷⁶ R.E. Hall,⁴⁸ L. Han,⁷ K. Hanagaki,⁵¹ K. Harder,⁶⁰ A. Harel,⁷² R. Harrington,⁶⁴ J.M. Hauptman,⁵⁸ R. Hauser,⁶⁶ J. Hays,⁵⁴ T. Hebbeker,²¹ D. Hedin,⁵³ J.G. Hegeman,³⁴ J.M. Heinmiller,⁵² A.P. Heinson,⁴⁹ U. Heintz,⁶³ C. Hensel,⁵⁹ K. Herner,⁷³ G. Hesketh,⁶⁴ M.D. Hildreth,⁵⁶ R. Hirosky,⁸² J.D. Hobbs,⁷³ B. Hoeneisen,¹² H. Hoeth,²⁶ M. Hohlfeld,¹⁶ S.J. Hong,³¹ R. Hooper,⁷⁸ P. Houben,³⁴ Y. Hu,⁷³ Z. Hubacek,¹⁰ V. Hynek,⁹ I. Iashvili,⁷⁰ R. Illingworth,⁵¹ A.S. Ito,⁵¹ S. Jabeen,⁶³ M. Jaffré,¹⁶ S. Jain,⁷⁶ K. Jakobs,²³ C. Jarvis,⁶² A. Jenkins,⁴⁴ R. Jesik,⁴⁴ K. Johns,⁴⁶ C. Johnson,⁷¹ M. Johnson,⁵¹ A. Jonckheere,⁵¹ P. Jonsson,⁴⁴ A. Juste,⁵¹ D. Käfer,²¹ S. Kahn,⁷⁴ E. Kajfasz,¹⁵ A.M. Kalinin,³⁶ J.M. Kalk,⁶¹ J.R. Kalk,⁶⁶ S. Kappler,²¹ D. Karmanov,³⁸ J. Kasper,⁶³ P. Kasper,⁵¹ I. Katsanos,⁷¹ D. Kau,⁵⁰ R. Kaur,²⁷ R. Kehoe,⁸⁰ S. Kermiche,¹⁵ N. Khalatyan,⁶³ A. Khanov,⁷⁷ A. Kharchilava,⁷⁰ Y.M. Kharzhev,³⁶ D. Khatidze,⁷¹ H. Kim,⁷⁹ T.J. Kim,³¹ M.H. Kirby,³⁵ B. Klima,⁵¹ J.M. Kohli,²⁷ J.-P. Konrath,²³ M. Kopal,⁷⁶ V.M. Korablev,³⁹ J. Kotcher,⁷⁴ B. Kothari,⁷¹ A. Koubarovsky,³⁸ A.V. Kozelov,³⁹ J. Kozminski,⁶⁶ D. Krop,⁵⁵ A. Kryemadhi,⁸² T. Kuhl,²⁴ A. Kumar,⁷⁰ S. Kunori,⁶² A. Kupco,¹¹ T. Kurča,^{20,*} J. Kvita,⁹ S. Lammers,⁷¹ G. Landsberg,⁷⁸ J. Lazoflores,⁵⁰ A.-C. Le Bihan,¹⁹ P. Lebrun,²⁰ W.M. Lee,⁵³ A. Leflat,³⁸ F. Lehner,⁴² V. Lesne,¹³ J. Leveque,⁴⁶ P. Lewis,⁴⁴ J. Li,⁷⁹ Q.Z. Li,⁵¹ J.G.R. Lima,⁵³ D. Lincoln,⁵¹ J. Linnemann,⁶⁶ V.V. Lipaev,³⁹ R. Lipton,⁵¹ Z. Liu,⁵ L. Lobo,⁴⁴ A. Lobodenko,⁴⁰ M. Lokajicek,¹¹ A. Lounis,¹⁹ P. Love,⁴³ H.J. Lubatti,⁸³ M. Lynker,⁵⁶ A.L. Lyon,⁵¹ A.K.A. Maciel,² R.J. Madaras,⁴⁷ P. Mättig,²⁶ C. Magass,²¹ A. Magerkurth,⁶⁵ A.-M. Magnan,¹⁴ N. Makovec,¹⁶ P.K. Mal,⁵⁶ H.B. Malbouisson,³ S. Malik,⁶⁸ V.L. Malyshev,³⁶ H.S. Mao,⁶ Y. Maravin,⁶⁰ M. Martens,⁵¹ R. McCarthy,⁷³ D. Meder,²⁴ A. Melnitchouk,⁶⁷ A. Mendes,¹⁵ L. Mendoza,⁸ M. Merkin,³⁸ K.W. Merritt,⁵¹ A. Meyer,²¹ J. Meyer,²² M. Michaut,¹⁸ H. Miettinen,⁸¹ T. Millet,²⁰ J. Mitrevski,⁷¹ J. Molina,³ N.K. Mondal,²⁹ J. Monk,⁴⁵ R.W. Moore,⁵ T. Moulik,⁵⁹ G.S. Muanza,¹⁶ M. Mulders,⁵¹ M. Mulhearn,⁷¹ L. Mundim,³ Y.D. Mutaf,⁷³ E. Nagy,¹⁵ M. Naimuddin,²⁸ M. Narain,⁶³ N.A. Naumann,³⁵ H.A. Neal,⁶⁵ J.P. Negret,⁸

P. Neustroev,⁴⁰ C. Noeding,²³ A. Nomerotski,⁵¹ S.F. Novaes,⁴ T. Nunnemann,²⁵ V. O'Dell,⁵¹ D.C. O'Neil,⁵ G. Obrant,⁴⁰ V. Oguri,³ N. Oliveira,³ N. Oshima,⁵¹ R. Otec,¹⁰ G.J. Otero y Garzón,⁵² M. Owen,⁴⁵ P. Padley,⁸¹ N. Parashar,⁵⁷ S.-J. Park,⁷² S.K. Park,³¹ J. Parsons,⁷¹ R. Partridge,⁷⁸ N. Parua,⁷³ A. Patwa,⁷⁴ G. Pawloski,⁸¹ P.M. Perea,⁴⁹ E. Perez,¹⁸ K. Peters,⁴⁵ P. Pétroff,¹⁶ M. Petteni,⁴⁴ R. Piegai,¹ J. Piper,⁶⁶ M.-A. Pleier,²² P.L.M. Podesta-Lerma,³³ V.M. Podstavkov,⁵¹ Y. Pogorelov,⁵⁶ M.-E. Pol,² A. Pompoš,⁷⁶ B.G. Pope,⁶⁶ A.V. Popov,³⁹ C. Potter,⁵ W.L. Prado da Silva,³ H.B. Prosper,⁵⁰ S. Protopopescu,⁷⁴ J. Qian,⁶⁵ A. Quadt,²² B. Quinn,⁶⁷ M.S. Rangel,² K.J. Rani,²⁹ K. Ranjan,²⁸ P.N. Ratoff,⁴³ P. Renkel,⁸⁰ S. Reucroft,⁶⁴ M. Rijssenbeek,⁷³ I. Ripp-Baudot,¹⁹ F. Rizatdinova,⁷⁷ S. Robinson,⁴⁴ R.F. Rodrigues,³ C. Royon,¹⁸ P. Rubinov,⁵¹ R. Ruchti,⁵⁶ V.I. Rud,³⁸ G. Sajot,¹⁴ A. Sánchez-Hernández,³³ M.P. Sanders,⁶² A. Santoro,³ G. Savage,⁵¹ L. Sawyer,⁶¹ T. Scanlon,⁴⁴ D. Schaile,²⁵ R.D. Schamberger,⁷³ Y. Scheglov,⁴⁰ H. Schellman,⁵⁴ P. Schieferdecker,²⁵ C. Schmitt,²⁶ C. Schwanenberger,⁴⁵ A. Schwartzman,⁶⁹ R. Schwienhorst,⁶⁶ J. Sekaric,⁵⁰ S. Sengupta,⁵⁰ H. Severini,⁷⁶ E. Shabalina,⁵² M. Shamim,⁶⁰ V. Shary,¹⁸ A.A. Shchukin,³⁹ W.D. Shephard,⁵⁶ R.K. Shivpuri,²⁸ D. Shpakov,⁵¹ V. Siccaldi,¹⁹ R.A. Sidwell,⁶⁰ V. Simak,¹⁰ V. Sirotenko,⁵¹ P. Skubic,⁷⁶ P. Slattery,⁷² R.P. Smith,⁵¹ G.R. Snow,⁶⁸ J. Snow,⁷⁵ S. Snyder,⁷⁴ S. Söldner-Rembold,⁴⁵ X. Song,⁵³ L. Sonnenschein,¹⁷ A. Sopczak,⁴³ M. Sosebee,⁷⁹ K. Soustruznik,⁹ M. Souza,² B. Spurlock,⁷⁹ J. Stark,¹⁴ J. Steele,⁶¹ V. Stolin,³⁷ A. Stone,⁵² D.A. Stoyanova,³⁹ J. Strandberg,⁴¹ S. Strandberg,⁴¹ M.A. Strang,⁷⁰ M. Strauss,⁷⁶ R. Ströhmer,²⁵ D. Strom,⁵⁴ M. Strovink,⁴⁷ L. Stutte,⁵¹ S. Sumowidagdo,⁵⁰ A. Sznajder,³ M. Talby,¹⁵ P. Tamburello,⁴⁶ W. Taylor,⁵ P. Telford,⁴⁵ J. Temple,⁴⁶ B. Tiller,²⁵ M. Titov,²³ V.V. Tokmenin,³⁶ M. Tomoto,⁵¹ T. Toole,⁶² I. Torchiani,²³ S. Towers,⁴³ T. Trefzger,²⁴ S. Trincaz-Duvold,¹⁷ D. Tsybychev,⁷³ B. Tuchming,¹⁸ C. Tully,⁶⁹ A.S. Turcot,⁴⁵ P.M. Tuts,⁷¹ R. Unalan,⁶⁶ L. Uvarov,⁴⁰ S. Uvarov,⁴⁰ S. Uzunyan,⁵³ B. Vachon,⁵ P.J. van den Berg,³⁴ R. Van Kooten,⁵⁵ W.M. van Leeuwen,³⁴ N. Varelas,⁵² E.W. Varnes,⁴⁶ A. Vartapetian,⁷⁹ I.A. Vasilyev,³⁹ M. Vaupel,²⁶ P. Verdier,²⁰ L.S. Vertogradov,³⁶ M. Verzocchi,⁵¹ F. Villeneuve-Seguié,⁴⁴ P. Vint,⁴⁴ J.-R. Vlimant,¹⁷ E. Von Toerne,⁶⁰ M. Voutilainen,^{68,†} M. Vreeswijk,³⁴ H.D. Wahl,⁵⁰ L. Wang,⁶² M.H.L.S Wang,⁵¹ J. Warchol,⁵⁶ G. Watts,⁸³ M. Wayne,⁵⁶ M. Weber,⁵¹ H. Weerts,⁶⁶ N. Wermes,²² M. Wetstein,⁶² A. White,⁷⁹ D. Wicke,²⁶ G.W. Wilson,⁵⁹ S.J. Wimpenny,⁴⁹ M. Wobisch,⁵¹ J. Womersley,⁵¹ D.R. Wood,⁶⁴ T.R. Wyatt,⁴⁵ Y. Xie,⁷⁸ N. Xuan,⁵⁶ S. Yacoob,⁵⁴ R. Yamada,⁵¹ M. Yan,⁶² T. Yasuda,⁵¹ Y.A. Yatsunenko,³⁶ K. Yip,⁷⁴ H.D. Yoo,⁷⁸ S.W. Youn,⁵⁴ C. Yu,¹⁴ J. Yu,⁷⁹ A. Yurkewicz,⁷³ A. Zatserklyaniy,⁵³ C. Zeitnitz,²⁶ D. Zhang,⁵¹ T. Zhao,⁸³ B. Zhou,⁶⁵ J. Zhu,⁷³ M. Zielinski,⁷² D. Zieminska,⁵⁵ A. Zieminski,⁵⁵ V. Zutshi,⁵³ and E.G. Zverev³⁸

(DØ Collaboration)

¹ Universidad de Buenos Aires, Buenos Aires, Argentina

² LAFEX, Centro Brasileiro de Pesquisas Físicas, Rio de Janeiro, Brazil

³ Universidade do Estado do Rio de Janeiro, Rio de Janeiro, Brazil

⁴ Instituto de Física Teórica, Universidade Estadual Paulista, São Paulo, Brazil

⁵ University of Alberta, Edmonton, Alberta, Canada, Simon Fraser University, Burnaby, British Columbia, Canada, York University, Toronto, Ontario, Canada, and McGill University, Montreal, Quebec, Canada

⁶ Institute of High Energy Physics, Beijing, People's Republic of China

⁷ University of Science and Technology of China, Hefei, People's Republic of China

⁸ Universidad de los Andes, Bogotá, Colombia

⁹ Center for Particle Physics, Charles University, Prague, Czech Republic

¹⁰ Czech Technical University, Prague, Czech Republic

¹¹ Center for Particle Physics, Institute of Physics, Academy of Sciences of the Czech Republic, Prague, Czech Republic

¹² Universidad San Francisco de Quito, Quito, Ecuador

¹³ Laboratoire de Physique Corpusculaire, IN2P3-CNRS, Université Blaise Pascal, Clermont-Ferrand, France

¹⁴ Laboratoire de Physique Subatomique et de Cosmologie, IN2P3-CNRS, Université de Grenoble 1, Grenoble, France

¹⁵ CPPM, IN2P3-CNRS, Université de la Méditerranée, Marseille, France

¹⁶ IN2P3-CNRS, Laboratoire de l'Accélérateur Linéaire, Orsay, France

¹⁷ LPNHE, IN2P3-CNRS, Universités Paris VI and VII, Paris, France

¹⁸ DAPNIA/Service de Physique des Particules, CEA, Saclay, France

¹⁹ IPHC, IN2P3-CNRS, Université Louis Pasteur, Strasbourg, France, and Université de Haute Alsace, Mulhouse, France

²⁰ Institut de Physique Nucléaire de Lyon, IN2P3-CNRS, Université Claude Bernard, Villeurbanne, France

²¹ III. Physikalisches Institut A, RWTH Aachen, Aachen, Germany

²² Physikalisches Institut, Universität Bonn, Bonn, Germany

²³ Physikalisches Institut, Universität Freiburg, Freiburg, Germany

²⁴ Institut für Physik, Universität Mainz, Mainz, Germany

²⁵ Ludwig-Maximilians-Universität München, München, Germany

²⁶ Fachbereich Physik, University of Wuppertal, Wuppertal, Germany

²⁷ Panjab University, Chandigarh, India

- ²⁸ Delhi University, Delhi, India
- ²⁹ Tata Institute of Fundamental Research, Mumbai, India
- ³⁰ University College Dublin, Dublin, Ireland
- ³¹ Korea Detector Laboratory, Korea University, Seoul, Korea
- ³² SungKyunKwan University, Suwon, Korea
- ³³ CINVESTAV, Mexico City, Mexico
- ³⁴ FOM-Institute NIKHEF and University of Amsterdam/NIKHEF, Amsterdam, The Netherlands
- ³⁵ Radboud University Nijmegen/NIKHEF, Nijmegen, The Netherlands
- ³⁶ Joint Institute for Nuclear Research, Dubna, Russia
- ³⁷ Institute for Theoretical and Experimental Physics, Moscow, Russia
- ³⁸ Moscow State University, Moscow, Russia
- ³⁹ Institute for High Energy Physics, Protvino, Russia
- ⁴⁰ Petersburg Nuclear Physics Institute, St. Petersburg, Russia
- ⁴¹ Lund University, Lund, Sweden, Royal Institute of Technology and Stockholm University, Stockholm, Sweden, and Uppsala University, Uppsala, Sweden
- ⁴² Physik Institut der Universität Zürich, Zürich, Switzerland
- ⁴³ Lancaster University, Lancaster, United Kingdom
- ⁴⁴ Imperial College, London, United Kingdom
- ⁴⁵ University of Manchester, Manchester, United Kingdom
- ⁴⁶ University of Arizona, Tucson, Arizona 85721, USA
- ⁴⁷ Lawrence Berkeley National Laboratory and University of California, Berkeley, California 94720, USA
- ⁴⁸ California State University, Fresno, California 93740, USA
- ⁴⁹ University of California, Riverside, California 92521, USA
- ⁵⁰ Florida State University, Tallahassee, Florida 32306, USA
- ⁵¹ Fermi National Accelerator Laboratory, Batavia, Illinois 60510, USA
- ⁵² University of Illinois at Chicago, Chicago, Illinois 60607, USA
- ⁵³ Northern Illinois University, DeKalb, Illinois 60115, USA
- ⁵⁴ Northwestern University, Evanston, Illinois 60208, USA
- ⁵⁵ Indiana University, Bloomington, Indiana 47405, USA
- ⁵⁶ University of Notre Dame, Notre Dame, Indiana 46556, USA
- ⁵⁷ Purdue University Calumet, Hammond, Indiana 46323, USA
- ⁵⁸ Iowa State University, Ames, Iowa 50011, USA
- ⁵⁹ University of Kansas, Lawrence, Kansas 66045, USA
- ⁶⁰ Kansas State University, Manhattan, Kansas 66506, USA
- ⁶¹ Louisiana Tech University, Ruston, Louisiana 71272, USA
- ⁶² University of Maryland, College Park, Maryland 20742, USA
- ⁶³ Boston University, Boston, Massachusetts 02215, USA
- ⁶⁴ Northeastern University, Boston, Massachusetts 02115, USA
- ⁶⁵ University of Michigan, Ann Arbor, Michigan 48109, USA
- ⁶⁶ Michigan State University, East Lansing, Michigan 48824, USA
- ⁶⁷ University of Mississippi, University, Mississippi 38677, USA
- ⁶⁸ University of Nebraska, Lincoln, Nebraska 68588, USA
- ⁶⁹ Princeton University, Princeton, New Jersey 08544, USA
- ⁷⁰ State University of New York, Buffalo, New York 14260, USA
- ⁷¹ Columbia University, New York, New York 10027, USA
- ⁷² University of Rochester, Rochester, New York 14627, USA
- ⁷³ State University of New York, Stony Brook, New York 11794, USA
- ⁷⁴ Brookhaven National Laboratory, Upton, New York 11973, USA
- ⁷⁵ Langston University, Langston, Oklahoma 73050, USA
- ⁷⁶ University of Oklahoma, Norman, Oklahoma 73019, USA
- ⁷⁷ Oklahoma State University, Stillwater, Oklahoma 74078, USA
- ⁷⁸ Brown University, Providence, Rhode Island 02912, USA
- ⁷⁹ University of Texas, Arlington, Texas 76019, USA
- ⁸⁰ Southern Methodist University, Dallas, Texas 75275, USA
- ⁸¹ Rice University, Houston, Texas 77005, USA
- ⁸² University of Virginia, Charlottesville, Virginia 22901, USA
- ⁸³ University of Washington, Seattle, Washington 98195, USA

(Dated: March 30, 2007)

We present a study of events with Z bosons and associated jets produced at the Fermilab Tevatron Collider in $p\bar{p}$ collisions at a center of mass energy of 1.96 TeV. The data sample consists of nearly 14,000 $Z/\gamma^* \rightarrow e^+e^-$ candidates corresponding to an integrated luminosity of 0.4 fb^{-1} collected with the DØ detector. Ratios of the $Z/\gamma^* + \geq n$ jet cross sections to the total inclusive Z/γ^* cross

section have been measured for $n = 1$ to 4 jets, and found to be in good agreement with a next-to-leading order QCD calculation and with a tree-level QCD prediction with parton shower simulation and hadronization.

PACS numbers: 13.38.Dg, 14.70.Hp, 13.87.-a, 12.38.Aw, 12.38.Qk, 13.85.-t

Leptonic decays of electroweak gauge bosons, W^\pm and Z , produced in association with jets are prominent signatures at present and future hadron colliders. Measurements of W (or Z) + $\geq n$ jet cross sections are important for understanding perturbative quantum chromodynamics (QCD) calculations and for developing Monte Carlo (MC) simulation programs capable of handling partons in the final state at leading order (LO), or, in some cases, next-to-leading order (NLO). Furthermore, the production of W or Z bosons with associated jets represents a significant background to Higgs boson searches, as well as to other standard model processes of interest, such as top quark production, and many searches for new phenomena at the Fermilab Tevatron Collider and at the CERN Large Hadron Collider.

Measurements of $Z + \geq n$ jet cross sections with lower integrated luminosity and at lower center of mass energy were performed previously by the CDF collaboration [1]. In this study, we present the first measurement of the fully corrected ratios of the $Z/\gamma^* + \geq n$ jet production cross sections to the total inclusive Z/γ^* cross section for jet multiplicities $n = 1 - 4$ in $p\bar{p}$ collisions at $\sqrt{s} = 1.96$ TeV. Cross section measurements based on inclusive jet multiplicities provide theoretically sound observables, and can be compared to a variety of predictions. Our results are based on a data sample corresponding to an integrated luminosity of 0.4 fb^{-1} accumulated with the DØ detector.

The elements of the DØ detector [2] of primary importance to this analysis are the uranium/liquid-argon sampling calorimeter and the tracking system. The DØ calorimeter has a granularity of $\Delta\eta \times \Delta\phi = 0.1 \times 0.1$, forming projective towers, where η is the pseudorapidity ($\eta = -\ln[\tan(\theta/2)]$, θ is the polar angle relative to the proton beam), and ϕ is the azimuthal angle. The calorimeter has a central section covering pseudorapidities up to ≈ 1.1 , and two end calorimeters that extend the coverage to $|\eta| \approx 4.2$. The tracking system consists of a silicon micro-strip tracker and a central fiber tracker, both located within a 2 T superconducting solenoidal magnet, with designs optimized for tracking and vertexing at pseudorapidities of $|\eta| < 3$ and $|\eta| < 2.5$, respectively.

The data sample for this analysis [3] was collected between April 2002 and June 2004. Events from $Z/\gamma^* \rightarrow e^+e^-$ decays were selected with a combination of single-electron triggers, based on energy deposited in calorimeter towers ($\Delta\eta \times \Delta\phi = 0.2 \times 0.2$). Final event selection was based on detector performance, event properties, and electron and jet identification criteria.

Events were required to have a reconstructed primary vertex with a position along the beam direction within 60 cm of the detector center. Electrons were reconstructed from electromagnetic (EM) clusters in the calorimeter using a simple cone algorithm. The two electron candidates in the event with the highest transverse momentum components relative to the beam direction (p_T), and both with $p_T > 25$ GeV, were used to reconstruct the Z boson candidate. The two electrons were required to be in the central region of the calorimeter $|\eta_{\text{det}}| < 1.1$ (pseudorapidity η_{det} is calculated relative to the center of the detector), and at least one required to fire the trigger(s) for the event. The electron pair also had to have an invariant mass consistent with the Z boson mass of $75 \text{ GeV} < M_{ee} < 105 \text{ GeV}$.

To reduce background (mainly from jets misidentified as electrons), the EM clusters were required to pass three quality criteria based on the shower profile: (i) the electron had to deposit at least 90% of its energy in the 21-radiation-length EM calorimeter (ii) the lateral and longitudinal shape of the energy cluster had to be consistent with those of an electron, and (iii) the electron had to be isolated from other energy deposits in the calorimeter, with an isolation fraction $f_{\text{iso}} < 0.15$. (The isolation fraction is defined as $f_{\text{iso}} = [E(0.4) - E_{\text{EM}}(0.2)]/E_{\text{EM}}(0.2)$, where $E(R_{\text{cone}})$ and $E_{\text{EM}}(R_{\text{cone}})$ are respectively the total and EM energies within a cone of radius $R_{\text{cone}} = \sqrt{(\Delta\eta)^2 + (\Delta\phi)^2}$ centered around the direction of the electron.) Additionally, at least one of the electrons was required to have a spatially matched track associated with the reconstructed calorimeter cluster, and the track momentum had to be consistent with the energy of the EM cluster. A total of 13,893 events passed the selection criteria.

Jets were reconstructed using the ‘‘Run II cone algorithm’’ [4] that combines particles within a cone of radius $R_{\text{cone}} = 0.5$. Spurious jets from isolated noisy calorimeter cells were eliminated through selections on patterns of jet energy deposition. Jets were required to be consistent with energy depositions measured at the trigger stage. This requirement was introduced to address precision readout noise problems: The jet energy at the Level 1 trigger tower level was compared to the jet energy derived from the jet cone algorithm, which was based on calorimeter cell precision readout. The transverse momentum of each jet was corrected for multiple $p\bar{p}$ interactions, calorimeter noise, out-of-cone showering effects, and energy response of the calorimeter as determined from the missing transverse energy balance of photon-jet events [5]. Jets were required to have

$p_T > 20$ GeV and $|\eta| < 2.5$, and were eliminated if they overlapped with electrons from Z boson decay within $\Delta R = \sqrt{(\Delta\eta)^2 + (\Delta\phi)^2} = 0.4$. Small losses of jets resulting from this separation criterion for electrons from Z boson decays were estimated as a function of the number of associated jets using a PYTHIA [6] MC sample.

The jet energy resolutions were derived from a measurement in photon+jet data for low jet energies and dijet data for higher jet energy values. Fits to the transverse energy asymmetry $[p_T(1) - p_T(2)]/[p_T(1) + p_T(2)]$ between the transverse momenta of the back-to-back jets and/or photon ($p_T(1)$ and $p_T(2)$) were then used to obtain the jet energy resolution as a function of jet rapidity and transverse energy. The largest contribution to the jet energy resolution uncertainty was due to limited statistics in the samples used.

The electron efficiencies for trigger, track matching, reconstruction, and identification were determined from data, based on a “tag-and-probe” method. Z candidates were selected with one electron (the tag) satisfying a tighter track-matching requirement to further reduce background contamination, and another electron (the probe) with all other criteria applied, except the one under study. The fraction of events with probe electrons passing the requirement under study determined the efficiency of a given criterion. The overall trigger efficiency for Z candidates that survived the analysis selections was found to be greater than 99%. The electron reconstruction and identification efficiencies were measured as a function of azimuthal angle and p_T , and the average efficiency was found to be about 89%. The combined spatial and energy track-matching efficiency was measured to be about 77%. The electron reconstruction, selection, trigger, and track-matching efficiencies were examined as a function of jet multiplicity. No significant variations of the efficiencies were observed, except for the track-matching efficiency, for which the multiplicity dependence was taken into account in correcting the data.

The kinematic and geometric acceptance for electrons from Z/γ^* decays in the mass region of $75 \text{ GeV} < M_{ee} < 105 \text{ GeV}$, for a primary vertex within 60 cm of the detector center, was determined as a function of jet multiplicity. An inclusive PYTHIA sample was used to calculate the acceptance for the inclusive Z/γ^* sample. The PYTHIA events were weighted so that the p_T distribution of the Z boson in the MC agreed with data. The jet multiplicity dependence of the acceptance was calculated using a $Z/\gamma^* + n$ parton leading-order generator [7], with the evolution of partons into hadrons carried out in PYTHIA. All the samples were processed through full DØ detector simulation using GEANT [8] and the DØ reconstruction software. The overall dielectron acceptance for the $Z/\gamma^* + \geq 4$ jet sample was found to be about 30% higher than the acceptance for the Z/γ^* inclusive sample, because events with jets tend to recoil from Z bosons of

larger p_T , and thereby produce decay products that are more likely to fall within the geometric acceptance.

The reconstruction and identification efficiency of jets was determined from a MC sample with full detector simulation, and processed through the same programs as the data. A scaling factor was applied to the MC jets to adjust their reconstruction and identification efficiency to that of jets in data, using the “ Z p_T -balance” method [9]. In events with Z candidates, a search was performed for a recoiling jet opposite in azimuth to the Z boson. The probability of finding a recoiling jet as a function of the p_T of the Z was measured in data and MC. The ratio of these probabilities defined the scaling factor that was applied to the MC jets. After applying the scaling factor, the jet reconstruction and identification efficiency was determined by matching particle-level jets (i.e., jets found from final-state generator-level particles, after parton hadronization) to calorimeter jets. The efficiency was parameterized as a function of the p_T of the particle-level jet, where the p_T values were smeared with jet energy resolutions observed in data, as measured in three η regions of the calorimeter. As a cross check, the scaling factor determined from the “ Z p_T -balance” method was compared to the scaling factor obtained for photon+jet events, and found to be consistent with one another.

The primary background to the Z/γ^* dielectron signal is from multijet production, in which the jets have a large electromagnetic component or they are mismeasured in some way that causes them to pass the electron selection criteria. We refer to this instrumental background as “QCD”. For the $Z/\gamma^* + \geq 0 - 2$ jet samples, a convoluted Gaussian/Breit-Wigner function was used to fit the Z lineshape, and an exponential form was used to account for both the QCD background and the Drell-Yan (γ^*) component of the signal. For the lower statistics $Z/\gamma^* + \geq 3$ jet sample, the contributions from QCD and Drell-Yan components were estimated from the side bands of the Z in the dielectron invariant mass spectrum. In each case, a PYTHIA sample was used to disentangle the QCD component from the Drell-Yan contribution. The background contribution for the $Z/\gamma^* + \geq 4$ jet multiplicity sample was estimated by extrapolating to $n = 4$ an exponential fit to the QCD background in the $0 - 3$ jet multiplicity bins. The background contribution from QCD processes was found to be 3 - 5%, depending on jet multiplicity. There are also contributions to Z/γ^* candidates that are not from misidentified electrons, but correspond to other standard model processes (e.g., $t\bar{t}$ production, $Z \rightarrow \tau^+\tau^-$, $W \rightarrow e\nu$). These small ($< 1\%$) irreducible background contributions were also taken into account in the analysis.

The cross sections as a function of jet multiplicity were corrected for jet reconstruction and identification efficiencies, and for event migration due to the finite jet energy resolution of the detector. The correction factors were determined using two independent MC sam-

TABLE I: Cross-section ratios (R_n) with statistical and systematic uncertainties (all $\times 10^{-3}$) for different inclusive jet multiplicities.

Multiplicity ($Z/\gamma^* + \geq n$ jets)	$n \geq 1$	$n \geq 2$	$n \geq 3$	$n \geq 4$
R_n	120.1	18.6	2.8	0.90
Total Statistical Uncertainty	± 3.3	± 1.4	± 0.56	± 0.44
Total Systematic Uncertainty	-17.1, +15.6	-5.0, +6.2	-1.06, +1.43	-0.40, +0.48
Jet Energy Calibration	± 11.7	± 3.3	± 0.74	± 0.23
Jet Reconstruction/Identification	-7.0, +2.2	-2.9, +4.3	-0.64, +0.82	-0.30, +0.40
Unsmearing Procedure	-3.6, +2.2	-1.6, +2.4	-0.24, +0.85	-0.08, +0.09
Jet Energy Resolution	-2.7, +3.4	-0.04, +0.13	-0.17, +0.15	-0.03, +0.04
Acceptance	± 1.8	± 0.7	± 0.10	± 0.003
Efficiencies (Trigger, EM, Track)	± 8.5	± 1.3	± 0.20	± 0.07
Electron-Jet-Overlap	± 3.2	± 0.7	± 0.14	± 0.05

ples, both tuned to match the measured inclusive jet multiplicity and jet p_T distributions in data. The first sample was based on PYTHIA simulations. The second sample (ME-PS) was based on MADGRAPH [10] $Z/\gamma^* + n$ LO Matrix Element (ME) predictions, using PYTHIA for parton showering (PS) and hadronization, and a modified CKKW [11] method to map the $Z/\gamma^* + n$ parton event into a parton shower history [12]. The ME-PS predictions relied on MADGRAPH tree-level processes of up to three partons. Both these samples contained only particle-level jets (i.e., no detector simulation). The p_T of the jets was smeared with the jet energy resolutions found in data. Subsequently, some jets were removed randomly from the sample, to simulate the measured jet reconstruction/identification efficiencies. The ratio of the two inclusive jet multiplicity distributions (the generated distribution and the one with the jet reconstruction/identification efficiency and energy resolution applied) determined the unsmearing correction factors for a given MC sample. The weighted averages of the correction factors corresponding to the two sets of MC procedures were applied as a function of jet multiplicity to correct the jet multiplicity spectrum in data. The differences between the correction factors for the two calculations contribute to the systematic uncertainty of the procedure. Another source of systematic uncertainty was determined from a closure test, and was estimated by applying the full unsmearing procedure to a MC control sample. The unsmearing correction factors range from 1.11 to 2.9 for ≥ 1 and ≥ 4 jets, respectively.

The fully corrected ratios, R_n , of the $Z/\gamma^* + \geq n$ jet production cross sections to the inclusive Z/γ^* cross section

$$R_n \equiv \frac{\sigma(Z/\gamma^* + \geq n \text{ jets})}{\sigma(Z/\gamma^*)} \quad (1)$$

for the mass region $75 \text{ GeV} < M_{ee} < 105 \text{ GeV}$ are summarized in Table I. Systematic uncertainties include contributions from jet energy calibration corrections, jet reconstruction and identification efficiency, the unsmearing procedure, jet energy resolution, and variations in

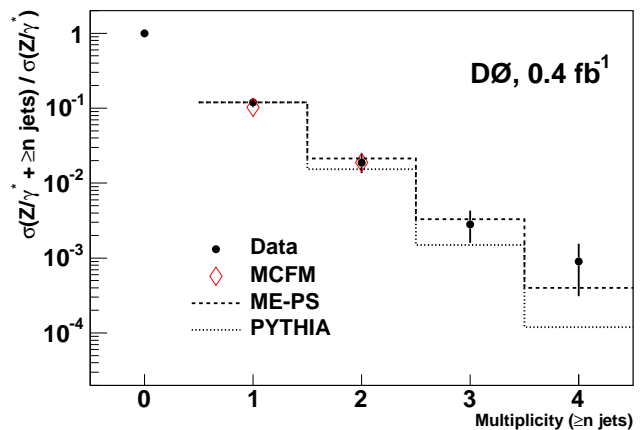


FIG. 1: Ratios of the $Z/\gamma^* + \geq n$ jet cross sections to the total inclusive Z/γ^* cross section versus jet multiplicity. The uncertainties on the data (dark circles) include the combined statistical and systematic uncertainties added in quadrature. The dashed line represents predictions of LO Matrix Element (ME) calculations using PYTHIA for parton showering (PS) and hadronization, normalized to the measured $Z/\gamma^* + \geq 1$ jet cross-section ratio. The dotted line represents the predictions of PYTHIA normalized to the measured $Z/\gamma^* + \geq 1$ jet cross-section ratio. The two open diamonds represent predictions from MCFM.

the acceptance for different event generators. They also take into account uncertainties in the variation of efficiencies for the trigger, electron reconstruction, identification, and track matching as a function of jet multiplicity, as well as uncertainties due to the electron-jet overlap correction. All these uncertainties are assumed to be uncorrelated, and are added in quadrature to estimate the total systematic uncertainty. The statistical uncertainties include contributions from the number of candidate events, background estimation, acceptance, efficiencies, and the unsmearing correction.

Figure 1 shows the fully corrected measured cross-section ratios for $Z/\gamma^* + \geq n$ jets as a function of jet multiplicity, compared to three QCD predictions.

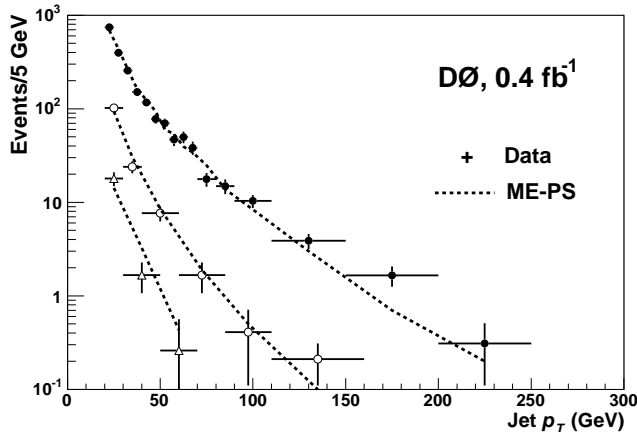


FIG. 2: Comparison between data and theory (ME-PS) for the highest p_T jet distribution in the $Z/\gamma^* + \geq 1$ jet sample (dark circles), for the second highest p_T jet distribution in the $Z/\gamma^* + \geq 2$ jet sample (open circles), and for the third highest p_T jet distribution in the $Z/\gamma^* + \geq 3$ jet sample (open triangles). The uncertainties on the data are only statistical. The MC distributions are normalized to the data.

MCFM [13] is a NLO calculation for up to $Z/\gamma^* + 2$ parton processes. CTEQ6M [14] parton distribution functions (PDF) were used in MCFM, and the factorization and renormalization scales μ_F , μ_R were both set to the Z boson mass, M_Z . Varying the PDF set and the renormalization/factorization scales to $M_Z^2 + p_{T,Z}^2$ had a minimal effect on the MCFM cross-section ratios. The ME-PS predictions are normalized to the measured $Z/\gamma^* + \geq 1$ jet cross-section ratio, and use the CTEQ6L PDF, with the factorization scale set to $\mu_F = M_Z$, and the renormalization scale set to $\mu_R = p_{T,jet}$ for jets from initial state radiation and $\mu_R = k_{T,jet}$ for jets from final state radiation ($k_{T,jet}$ is the transverse momentum of a radiated jet relative to its parent parton momentum). The PYTHIA predictions are also normalized to the measured $Z/\gamma^* + \geq 1$ jet cross-section ratio. Here, CTEQ5L [15] PDFs are used, and the factorization and renormalization scales are set to $\mu_F = \mu_R = M_Z$. The MCFM and ME-PS predictions are generally in good agreement with the data. PYTHIA predicts fewer events at high jet multiplicity because of missing higher order contributions at the hard-scatter level.

Figure 2 compares jet p_T spectra of the n^{th} jet, $n = 1, 2, 3$, in $Z/\gamma^* + \geq n$ jet events to the ME-PS MC predictions. The MC events have been passed through the full detector simulation, and the jet p_T spectra normalized separately to the data distributions. Good agreement can be seen over a wide range of jet transverse momenta.

In summary, we have presented the first measurements of fully corrected ratios of the $Z/\gamma^* + \geq n$ jet ($n = 1 - 4$) production cross sections to the total inclusive Z/γ^* cross section in $p\bar{p}$ collisions at $\sqrt{s} = 1.96$ TeV. The measured

ratios were found to be in good agreement with MCFM and an enhanced leading-order matrix element prediction with PYTHIA-simulated parton showering and hadronization. PYTHIA simulations alone appear to exhibit a deficit in high jet multiplicity events.

We thank S. Mrenna for providing us the ME-PS MC sample. We thank the staffs at Fermilab and collaborating institutions, and acknowledge support from the DOE and NSF (USA); CEA and CNRS/IN2P3 (France); FASI, Rosatom and RFBR (Russia); CAPES, CNPq, FAPERJ, FAPESP and FUNDUNESP (Brazil); DAE and DST (India); Colciencias (Colombia); CONACyT (Mexico); KRF and KOSEF (Korea); CONICET and UBACyT (Argentina); FOM (The Netherlands); PPARC (United Kingdom); MSMT (Czech Republic); CRC Program, CFI, NSERC and WestGrid Project (Canada); BMBF and DFG (Germany); SFI (Ireland); The Swedish Research Council (Sweden); Research Corporation; Alexander von Humboldt Foundation; and the Marie Curie Program.

[*] On leave from IEP SAS Kosice, Slovakia.

[†] Visitor from Helsinki Institute of Physics, Helsinki, Finland.

[‡] Visitor from Lewis University, Romeoville, IL, USA

- [1] F. Abe *et al.* (CDF Collaboration), Phys. Rev. Lett. **77**, 448 (1996).
- [2] V. Abazov *et al.* (D0 Collaboration), Nucl. Instrum. Meth. A **565**, 463 (2006).
- [3] M. Buehler, Ph.D. Dissertation, University of Illinois at Chicago, Fermilab-Thesis-2005-42 (2005).
- [4] G.C. Blazey *et al.*, in Proceedings of the Workshop: “QCD and Weak Boson Physics in Run II,” edited by U. Baur, R.K. Ellis, and D. Zeppenfeld, p. 47, Fermilab-Pub-00/297 (2000).
- [5] V. Abazov *et al.* (D0 Collaboration), Phys. Rev. D **74**, 092005 (2006).
- [6] T. Sjöstrand, Computer Physics Commun. **135**, 238 (2001).
- [7] M.L. Mangano, M. Moretti, F. Piccinini, R. Pittau, and A. Polosa, J. High Energy Phys. **07**, 001 (2003).
- [8] R. Brun and F. Carminati, CERN Program Library Long Writeup W5013, 1993 (unpublished).
- [9] J.M. Heinmiller, Ph.D. Dissertation, University of Illinois at Chicago, Fermilab-Thesis-2006-30 (2006).
- [10] F. Maltoni and T. Stelzer, J. High Energy Phys. **0302**, 027 (2003).
- [11] S. Catani, F. Krauss, R. Kuhn and B. R. Webber, J. High Energy Phys. **0111**, 063 (2001).
F. Krauss, J. High Energy Phys. **0208**, 015 (2002).
- [12] S. Mrenna and P. Richardson, J. High Energy Phys. **0405**, 040 (2004).
- [13] J. Campbell and R.K. Ellis, Phys. Rev. D **65**, 113007 (2002).
- [14] J. Pumplin *et al.*, J. High Energy Phys. **0207**, 12 (2002).
- [15] H.L. Lai *et al.*, Eur. Phys. J. **C12**, 375 (2000).